

# **Functional Brain Network Identification in Opioid Use Disorder Using Machine Learning Analysis of Resting-State fMRI BOLD Signals**

Ahmed Temtam<sup>a</sup>, Megan A. Witherow<sup>a</sup>, Liangsuo Ma<sup>b,c</sup>, M. Shibly Sadique<sup>a</sup>, F. Gerard Moeller<sup>b,c,d,e,f</sup>, and Khan M. Iftexharuddin<sup>\*a,g</sup>

<sup>a</sup> Vision Lab, Dept. of Electrical Engineering, Old Dominion University, Norfolk, VA, USA

<sup>b</sup> Institute of Drug and Alcohol Studies, Richmond, VA, USA

<sup>c</sup> Department of Psychiatry, Virginia Commonwealth University, Richmond, VA, USA

<sup>d</sup> Department of Pharmacology and Toxicology, Virginia Commonwealth University, VA, USA

<sup>e</sup> Department of Neurology, Virginia Commonwealth University, VA, USA

<sup>f</sup> C. Kenneth and Dianne Wright Center for Clinical and Translational Research, Virginia Commonwealth University, VA, USA

<sup>g</sup> Data Science Institute, Old Dominion University, Virginia Beach, VA, USA

\* Corresponding Author (email: [kiftekha@odu.edu](mailto:kiftekha@odu.edu))

## **Abstract**

Understanding the neurobiology of opioid use disorder (OUD) using resting-state functional magnetic resonance imaging (rs-fMRI) may help inform treatment strategies to improve patient outcomes. Recent literature suggests temporal characteristics of rs-fMRI blood oxygenation level-dependent (BOLD) signals may offer complementary information to functional connectivity analysis. However, existing studies of OUD analyze BOLD signals using measures computed across all time points. This study, for the first time in the literature, employs data-driven machine learning (ML) modeling of rs-fMRI BOLD features representing multiple time points to identify region(s) of interest that differentiate OUD subjects from healthy controls (HC). Following the triple network model, we obtain rs-fMRI BOLD features from the default mode network (DMN), salience network (SN), and executive control network (ECN) for 31 OUD and 45 HC subjects. Then, we use the Boruta ML algorithm to identify statistically significant BOLD features that differentiate OUD from HC, identifying the DMN as the most salient functional network for OUD. Furthermore, we conduct brain activity mapping, showing heightened neural activity within the DMN for OUD. We perform 5-fold cross-validation classification (OUD vs. HC) experiments to study the discriminative power of functional network features with and without fusing demographic features. The DMN shows the most discriminative power, achieving mean AUC and F1 scores of 80.91% and 73.97%, respectively, when fusing BOLD and demographic features. Follow-up Boruta analysis using BOLD features extracted from the medial prefrontal cortex, posterior cingulate cortex, and left and right temporoparietal junctions reveals significant features for all four functional hubs within the DMN.

**Keywords**—opioid use disorder, resting-state fMRI, machine learning, functional brain networks, default mode network, salience network, executive control network

## 1. Introduction

According to the Centers for Disease Control and Prevention, drug overdose deaths in the United States have exceeded 932,000 since 1999, and in 2020, about 75% of these deaths have been attributed to opioid use disorder (OUD) [1-3]. Given the substantial healthcare and societal costs associated with this public health crisis, understanding the neurobiology of OUD is of critical importance to improve patient outcomes. Research on the neurobiology underlying OUD has been instrumental to the development of current management strategies [4]. However, there are many open questions and the prognosis for patients with OUD remains poor, underscoring the need for continued study [4]. Machine learning (ML)-enabled data-driven analyses of resting-state functional magnetic resonance imaging (rs-fMRI) blood oxygenation level-dependent (BOLD) signals may prove promising for studying the neurobiology underlying OUD in humans [5, 6].

Various methods have been employed to investigate the functional neurobiology of OUD, including task-based fMRI [7] and rs-fMRI [8-11]. Task-based fMRI studies compare the BOLD signal at baseline with the BOLD signal in response to a cue, e.g., a drug or non-drug reward [7]. For example, the voxel-wise percentage change in the BOLD signal compared to the baseline may be used as a neural activity measure to identify brain regions involved in task-elicited cognitive processes [12]. Group-based analyses may then be performed to understand how the neural activity of OUD patients compares to healthy controls (HC). Studies using rs-fMRI measure spontaneous neural activity while the patients are at rest. Rather than focusing on neural activity within networks, studies of rs-fMRI have mostly investigated group differences in functional connectivity (FC) among multiple brain networks using various methods [7]. Traditional seed-based FC analyses are concerned with the relationship between the mean BOLD signal in the seed region of the brain and other voxels in the brain [13-16]. Such seed-based analyses are typically computed across all time points of the scan [17]. To study the temporal coherence of functional networks, independent component analysis has been proposed [18-21]. Functional networks may also be represented as a graph constructed by down sampling the voxels into nodes and building an adjacency matrix based on the correlations among all possible pairs of nodes [22, 23]. Thus, graph-based analysis may be used to investigate the local and global properties of functional networks across the brain [22, 23].

Few rs-fMRI studies [24, 25] have studied the neural activity within brain networks for OUD. Such studies [24, 25] use the amplitude of low frequency BOLD fluctuations (ALFF) to measure spontaneous neural activity in OUD, which is a static measure computed based on all time points. Recently, the variability of the BOLD signal in rs-fMRI has been suggested as a potential marker characterizing the integrity of neural systems, with increased variability being associated with compensatory or suboptimal functioning [26]. However, there has been limited work comparing FC analysis and BOLD variability [26]. In a recent rs-fMRI study on the effect of normative aging on the brain [26], significant BOLD variability is reported for older vs. younger adults while no difference is found in FC. Therefore, studying the characteristics of the BOLD signal within functional networks may reveal new and complementary insights into the functional mechanisms underlying brain changes associated with OUD. We expect that ML methods, which excel at learning complex patterns and nonlinear relationships, may prove promising for BOLD signal

analysis for OUD.

The literature has identified several key regions that may be of interest for studying the neurobiology underlying OUD. The triple network model (Fig. 1) is a framework describing the organization of three core neurocognitive networks in the human brain, i.e., the default mode network (DMN), salience network (SN), and executive control network (ECN), and how abnormal function among these three networks underlies multiple disorders in psychopathology, including substance use disorders [28, 29]. For example, in substance use disorders, processing may be biased towards the DMN rather than the ECN as a result of the SN assigning greater salience to substance-induced rewards [6]. However, until recently, few studies have explored the functional activity of individuals with OUD within the context of the triple network model [6]. Some studies [15, 18, 20] indicate a decrease in FC within the DMN, while others [21] report an increase. Additional investigations extend to the SN and ECN, revealing diverse patterns in connectivity. Notably, studies [15, 18, 20, 23, 27] demonstrate heightened neural responses to heroin-related cues among those with OUD, encompassing regions such as the parietal, limbic, frontal cortical, and midbrain areas. Within the DMN, functional hubs such as the medial prefrontal cortex (mPFC), posterior cingulate cortex (PCC), and the left and right temporoparietal junctions (lTPJ and rTPJ, respectively) have also been implicated in the neurobiology of OUD. For example, individuals with OUD have been shown to have decreased BOLD responses in the PCC when presented with non-drug rewards [30]. Short-term opioid abstiners have shown heightened activity in the mPFC [31] and PCC [14] compared to long-term abstiners. Individuals with OUD have also been reported to exhibit cortical thinning, which has been associated with connectivity changes [32, 33], extending into lTPJ and rTPJ [34].

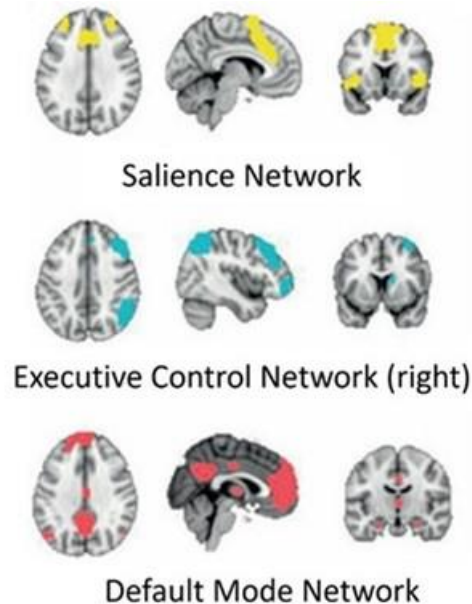


**Fig. 1.** Triple network model for localization of the SN (yellow), the ECN (blue), and DMN (red) [28].

ML is suitable for a broad range of applications in clinical research, including identifying patterns in patient datasets [35-40], assisting in biomarker discovery [41, 42], and developing predictive models [36, 37, 39, 43] that may contribute to more precise risk assessments and

prognoses. In the context of OUD, ML has been applied for drug repurposing to support treatment development [44, 45] and classification tasks to identify individuals with or at risk for opioid dependence and associated complications based on records data. In [35] and [46], the Random Forest ML algorithm has been used to predict opioid substance dependence based on electronic health records and National Survey on Drug Use and Health data, respectively. Commercial claims data has been used to predict patient overdose status using the Gradient Boosting Trees algorithm in [38] and risk of buprenorphine treatment discontinuation using multiple machine learning algorithms, including Random Forest, in [47]. However, to our knowledge, ML for rs-fMRI BOLD signal analysis and functional brain network mapping in OUD has yet to be explored.

Given its statistical foundation and stability [48], the Boruta ML algorithm [49] has proven to be a powerful tool for clinical research (e.g., biomarker discovery [41, 42], gene expression [50, 51], etc.). Recently, the Boruta algorithm has been used to analyze rs-fMRI FC patterns of individuals diagnosed with autism [52], attention-deficit/hyperactivity disorder (ADHD) [53, 54], and glioblastoma [55]. For example, in [52], Boruta identifies the DMN as a differentiated functional network in ASD and in [54], the DMN, attention network, auditory network, and others are identified by Boruta as differentiated functional networks in ADHD. Following the identification of important functional networks or regions of interest (ROIs), subsequent ML classification studies may be performed to provide further insight into the discriminative power of functional network features in distinguishing between patients with a particular diagnosis and HC [52, 55, 56]. To our knowledge, the Boruta ML algorithm has not yet been used to analyze functional networks in patients with OUD.

This study is the first in the literature to introduce a ML modeling utilizing rs-fMRI BOLD signal analysis to identify ROIs representing areas of differentiated neural activity for OUD within functional brain networks including DMN, SN, and ECN. While most rs-fMRI studies of OUD examine FC or neural activity using ALFF, the temporal characteristics of the BOLD signal have been underexamined. For example, BOLD variability has recently been suggested as a potential marker of neural system integrity [26]. Therefore, we adopt a data-driven ML approach to BOLD signal analysis for OUD. Our BOLD network features and ML-based modeling include temporal information from resting-state pseudo-events (e.g., blinking) across multiple time points, which has not been explicitly analyzed in other works. We perform follow-up Boruta analysis on functional hubs within the DMN, including the mPFC, PCC, ITPJ, and rTPJ. To study the discriminative power of the DMN, SN, and ECN, we perform multiple ML classification (OUD vs. HC) experiments using the BOLD functional brain network features with and without incorporating demographic features via feature fusion. Our comparison of OUD classification performance between models trained with DMN, SN, and ECN features reinforces the importance of the DMN in understanding the neurobiology of OUD.

## 2. Methods

Figure 2 shows our overall pipeline for rs-fMRI BOLD signal analysis, ROI identification, brain mapping and visualization (Fig. 2 (a)) and machine learning classification experiments to study

the discriminative power of functional networks (Fig. 2 (b)). In the following sections, we describe the details of the proposed method.

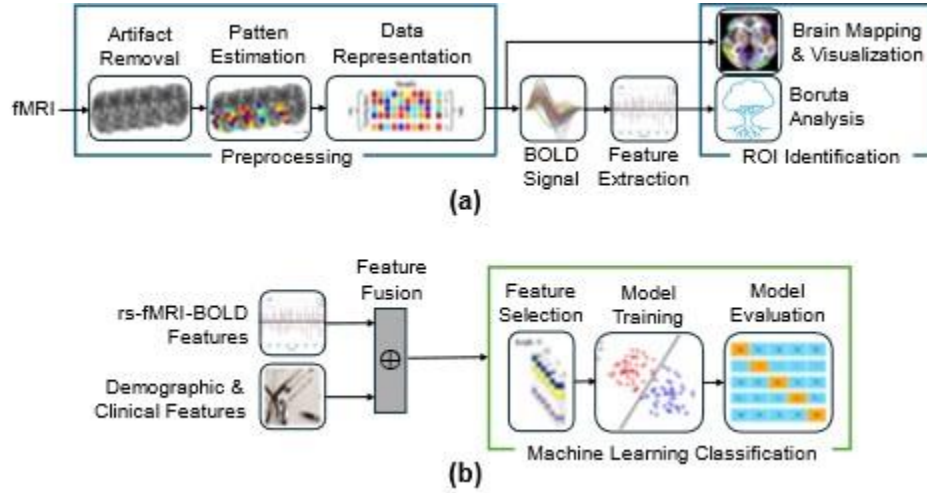


**Fig. 2.** Overall pipeline for rs-fMRI BOLD signal analysis, ROI identification, brain mapping and visualization, and machine learning experiments.

## 2.1 Dataset

This work acquires clinical and high-resolution rs-fMRI data from a National Institute on Drug Abuse (NIDA) study aimed at assessing the feasibility and validation of the Phenotyping Assessments Battery (PhAB) in non-intoxicated drug users. The NIDA study has been approved by the Committee for the Protection of Human Subjects and Institutional Review Board (IRB) of Virginia Commonwealth University under IRB number HM20023630 and has been performed in accordance with the Code of Ethics of the World Medical Association [57]. This study is conducted as a partnership between the Department of Drug and Alcohol Studies at Virginia Commonwealth University and the Vision Lab at Old Dominion University. The total number of subjects is  $n = 76$ . Table 1 provides the diagnostic (OUD or HC) breakdown of the subjects by gender. Table 2 describes the demographic features collected for these subjects.

**Table 1**  
Dataset Distribution

Subjects	Male	Female	Total	Mean Age
HC	21	24	45	33.8
OUD	18	13	31	39.6
Total	39	37	76	

**Table 2**  
Demographic Features

<b>Patient Demographics</b>	
<b>ETHNICITY</b>	Ethnicity of the subject
<b>EDUCATION (years)</b>	Subject’s number of years of education
<b>SEX</b>	Sex of the subject
<b>AGE (years)</b>	Subject’s age at the time of the scan
<b>HEIGHT (inches)</b>	Height of the subject in inches
<b>WEIGHT (lbs)</b>	Weight of the subject in pounds
<b>HANDEDNESS</b>	Dominant hand of the subject

## 2.2 Preprocessing and Feature Extraction

As described in [58], the rs-fMRI data undergo several preprocessing steps including elimination of signal artifacts (including those due to head motion, cardiac and respiratory extraneous signals) and pattern estimation to identify regions of neural activity which are organized into a data representation for subsequent analysis. Next, we extract features representing neural activity from the rs-fMRI BOLD signal. The BOLD contrast mechanism captures both neural activity (our target quantity) [59, 60] and the hemodynamic response, the brain's physiological reaction to neural activation [61-63]. To isolate the neural response from the hemodynamic response [64], the resting-state hemodynamic response function (rsHRF) [65, 66] is used to recover the onsets of pseudo-events triggering a hemodynamic response from the voxel-wise signal in the rs-fMRI BOLD data [21]. As the rsHRF represents the sequence of physiological changes that occur in the brain following neural activation [59, 63], the convolution of the rsHRF with the timing and duration of the events yields the predicted BOLD response. Comparing this predicted response to the observed BOLD signal reveals the extent to which the pseudo-events have influenced brain activity, yielding a set of features that estimate the underlying neural activity [67]. Following this approach, we extract  $p$  features from the BOLD signal data associated with each of the three functional brain networks (DMN, SN, and ECN).

## 2.3 Boruta ML Algorithm for ROI Identification

The Boruta algorithm is an ML approach for ‘all-relevant’ feature selection originally developed for research in genetics where features may be correlated [49], which is also to be expected for our rs-fMRI BOLD features [68]. The Boruta algorithm builds a statistical framework around the Random Forest ML algorithm to assess feature importance [49]. For a specified Type I error rate  $\alpha$ , all significantly discriminative features, e.g., for distinguishing between patients with OUD and HC, are identified based on statistical tests [49]. The Boruta algorithm produces highly stable feature selections and does not require samples to be independent or normally distributed [48, 49].

To investigate the contributions of the DMN, SN, and ECN to the differential neurobiology of OUD as compared to HC, we apply the Boruta algorithm to features extracted from each of these three functional brain networks. Building upon [49], our specific approach is as follows. First, we build our information system by joining the  $p$  DMN features,  $p$  SN features, and  $p$  ECN features on the index of the  $n = 76$  subjects to form a data matrix with shape  $n$  samples  $\times$   $3p$  features. Each of the  $n = 76$  samples is associated with a label, either ‘OUD’ or ‘HC’, which is encoded in

a separate label vector. Next, we make  $m$  copies of the data matrix. In these copies, we permute the sample values within each feature column to yield randomized ‘shadow features’, which will be used as references for assessing the significance of the original, unpermuted features. We join the  $n \times 3p$  data matrix and its  $m$  permuted replicates to form the extended information system with shape  $n \times (3 + m)p$ . Then, the following steps are repeated until the significance of each of the features is determined or a maximum number of iterations is reached:

1. Run the random forest algorithm on the extended information system to obtain feature importances for the features and shadow features with respect to their relative contributions in minimizing the OUD vs. HC classification loss.
2. Compare the importance of each feature to the  $c$ th percentile of the shadow features’ importance. Following [69], we select the value of  $c$  to account for chance correlations between the permuted shadow features and diagnostic labels (OUD or HC), which may occur depending upon the dataset size. Features with a higher importance than the  $c$ th percentile of the shadow features’ importance are assigned a ‘hit’.
3. Assign p-values to each of the features using the Binomial distribution at the end of each iteration (e.g., with the null hypothesis  $H_0: \eta = 0.5$ , where  $\eta$  is the probability of a hit, a feature may be assigned  $h$  hits in  $t$  Bernoulli trials (iterations)). We perform one-tailed binomial tests to confirm ( $H_0: \eta > 0.5$ ) important/significant features and reject ( $H_0: \eta < 0.5$ ) unimportant features. P-values are Bonferroni-corrected to account for multiple testing. Confirmed and rejected features are removed from the information system before continuing with the next iteration.

To conduct our analysis, we use the BorutaPy library ([https://github.com/scikit-learn-contrib/boruta\\_py/](https://github.com/scikit-learn-contrib/boruta_py/)) with the following settings: maximum of 1000 iterations, maximum tree depth of 5, and dynamic selection of the value of  $m$  and the number of trees in the ensemble at each iteration based on the number of features in the information system. From the Boruta algorithm, we obtain significant or not significant designations for each of features and their associated importance rankings. For each of the three functional networks (DMN, SN, and ECN), we use the percentage of significant features out of  $p$ , the total number of features extracted from each network, to select ROI(s) and evaluate the saliency of each functional network in distinguishing patients with OUD from HC. We also report the average feature rankings to further assess the relative importance of each of the three functional networks. In follow-up analysis, we use the Boruta algorithm to assess the relative importances of the functional hubs within the DMN, including the mPFC, PCC, ITPJ, and rTPJ.

#### *2.4 Brain Mapping and Visualization*

Brain activity mapping is pursued for visualization and as a second method for identifying the functional network(s) exhibiting heightened activity associated with OUD. We apply group analysis to systematically identify and characterize consistent patterns of neural activity across individuals within the context of OUD. The group analysis is performed using SPM for both OUD and HC classes and then utilizes automated anatomical labeling atlas 3 (AAL3) [70] to localize clusters of significant voxels to anatomically defined brain regions. This enables us to pinpoint specific brain regions with increased neural activity for OUD subjects.



## 2.5 ML Models for OUD vs. HC Classification

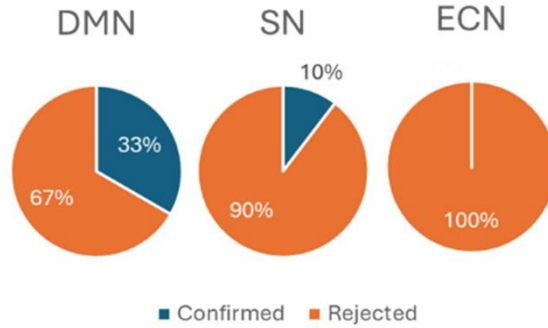
We study the discriminative power of the BOLD features from each of the functional brain networks by performing multiple ML classification experiments. Four different ML models are considered, including an SVM Classifier, Decision Tree, AdaBoost Classifier, and Random Forest Classifier, which, in our preliminary work [43], are found to be reasonable selections for OUD vs. HC classification using rs-fMRI BOLD features. We use an automated model selection process to identify the most effective classifier and associated hyperparameters among these options. The Scikit-learn library (<https://scikit-learn.org/>) is used to implement our approach.

Figure 2 (b) shows the pipeline for the proposed ML classification experiments. We consider rs-fMRI BOLD features extracted from each of the three functional networks (DMN, SN, ECN) as separate feature sets. For each feature set, we use the Least Absolute Shrinkage and Selection Operator (LASSO) approach to perform feature selection. The selected features are used to perform classification to differentiate OUD participants from HC subjects. We perform 5-fold cross-validation to assess the performance of models trained using each of the feature sets (DMN, SN, and ECN). To investigate the discriminative power of each of the functional networks with additional demographic information, we also perform experiments where we fuse the rs-fMRI BOLD feature sets with the demographic features in Table 2. Our validation set for model selection and hyperparameter tuning is obtained by randomly sampling 20% of the training data for each cross-validation train/test split. We perform model selection based on the validation performance with and without fusing the demographic features in Table 2. The best classifier across the three functional networks (DMN, ECN, SN) is used to assess the discriminative power of each functional network based on the held-out cross-validation test sets.

## 3. Results

### 3.1 Functional Brain Networks as ROIs for OUD

Figure 3 shows the Boruta ML analysis results with the percentages of features identified as significant and rejected as unimportant for each of the three functional networks (DMN, SN, and ECN) given a Type I error rate of  $\alpha = 0.05$ . With 33% of its features identified as significant (p-values  $< 0.05$ ), the DMN is the most salient of the three functional networks in distinguishing between OUD and HC. We find that the second most important network is the SN with 10% of its features identified as significant, while none of the features extracted from the ECN meet the cutoff for statistical significance. Table 3 reports the mean and standard deviation of the feature rankings (rank 1 being the best) for each network.



**Fig. 3.** Percentages of confirmed (significant,  $p$ -value  $< 0.05$ ) and rejected features for DMN, SN, and ECN functional networks based on our analysis using the Boruta ML algorithm.

**Table 3**

Mean and Standard Deviation (Std.) of Feature Importance Rankings (Lower is Better) for DMN, SN, and ECN Features

Network	Mean	Std.
DMN	34.71	37.13
SN	52.27	34.67
ECN	71.98	36.47

These findings are corroborated by brain mapping and visualization based on group analysis, as well as in the literature on FC and ALFF in OUD [14, 15, 18, 20] (further discussed in Section 4). Using a threshold of 0.001 for OUD subjects, we overlay brain activity clusters obtained from different subcortical areas (DMN, SN, and ECN) onto standard structural brain images for visualization. The results are presented in Fig. 4 for an example OUD case, where significant clusters in specific subcortical areas are highlighted in red. In Fig. 5 and Fig. 6, the green voxels indicate group analysis results illustrating brain activity for OUD and HC, respectively. Figure 5 highlights the DMN’s prominence in the neural activity of the OUD patients. Given the results based on our analysis with the Boruta ML algorithm and brain mapping, we select the DMN as the ROI for subsequent study. To evaluate the DMN’s discriminative power compared to the SN and ECN, we perform multiple OUD vs. HC classification experiments. We also conduct follow-up Boruta algorithm analysis of functional hubs within the DMN.

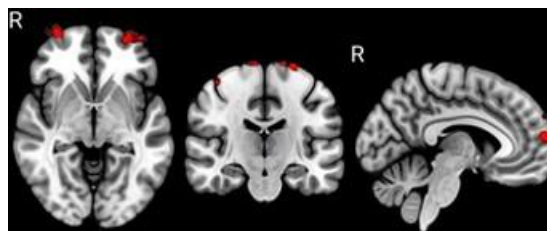


**Fig. 4.** Overlay of rs-fMRI BOLD for a representative OUD case over standard structural brain images, with significant clusters in specific subcortical areas displayed in red.

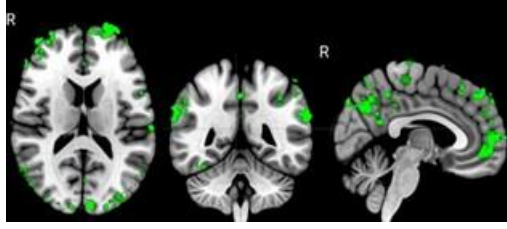


Fig. 5. Group analysis showing brain activity for OUD.

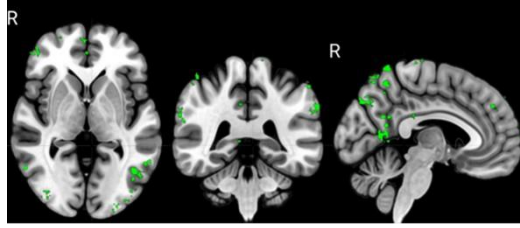


Fig. 6. Group analysis showing brain activity for HC.

### 3.2 Discriminative Power of Functional Network Features for OUD Classification

The results of our automatic model selection process are shown in Table 4. Since the F1 score considers class imbalance and the calibration of the decision boundary, we use the validation F1 score to select the best model for each BOLD feature set (DMN features, SN features, and ECN features, with and without fusing demographic features). Considering the BOLD functional network features only, the best OUD vs. HC classifier is AdaBoost when training with the DMN features. Decision Tree performs the best when using SN and ECN features. Fusing the demographic features with functional network features, SVM performs the best for all (DMN, SN, and ECN) feature sets. The hyperparameter selections for each of the classifiers are as follows. For SVM, we use the sigmoid kernel with  $C = 10$  and the default value of gamma, i.e.,  $\text{gamma} = 1 / (\text{number of features} \times \text{variance computed over the training data})$ . For Decision Tree and Random Forest, we set the maximum tree depth to 12. There are ten estimators in the ensembles for AdaBoost and Random Forest.

**Table 4**

Validation F1 Score (Mean  $\pm$  Std.) for SVM, Decision Tree, AdaBoost, and Random Forest Classifiers trained using DMN, SN, and ECN Features With and Without Fusing Demographic Features

Classifier	BOLD Features Only			BOLD Features Fused with Demographic Features		
	DMN	SN	ECN	DMN	SN	ECN
<b>SVM</b>	56.63% $\pm$ 12.99%	44.89% $\pm$ 20.92%	33.23% $\pm$ 14.57%	<b>80.21%</b> $\pm$ 7.15%	<b>77.02%</b> $\pm$ 6.62%	<b>77.09%</b> $\pm$ 13.14%
<b>Decision Tree</b>	52.70% $\pm$ 9.89%	<b>47.95%</b> $\pm$ 14.51%	<b>49.67%</b> $\pm$ 9.07%	55.00% $\pm$ 10.00%	42.67% $\pm$ 24.44%	51.56% $\pm$ 12.44%
<b>AdaBoost</b>	<b>60.19%</b> $\pm$ 5.47%	39.23% $\pm$ 10.34%	33.21% $\pm$ 13.18%	63.33% $\pm$ 9.41%	55.72% $\pm$ 12.11%	62.27% $\pm$ 13.80%
<b>Random Forest</b>	50.57% $\pm$ 9.36%	24.44% $\pm$ 14.74%	23.33% $\pm$ 15.87%	74.22% $\pm$ 9.44%	73.67% $\pm$ 10.35%	71.83% $\pm$ 10.10%

Our 5-fold cross-validation results based on training the selected best classifier for each set of BOLD functional network features (AdaBoost for DMN, Decision Tree for SN, and Decision Tree for ECN) are reported in Table 5. The DMN provides the greatest discriminative power, with the model trained on the DMN features (AUC 69.74%, F1 score 55.85%) outperforming models trained on SN features (AUC 47.14%, F1 score 39.20%) and ECN features (AUC 54.15%, F1 score 42.85%) across all metrics.

**Table 5**  
5-Fold Cross-validation Accuracy, Area under the ROC Curve (AUC), and F1 Scores for Models Trained on DMN, SN, and ECN Features

<b>Metric/Network</b>	<b>DMN</b>	<b>SN</b>	<b>ECN</b>
<b>Accuracy, Mean <math>\pm</math> Std.</b>	63.00% $\pm$ 7.33%	46.00% $\pm$ 8.00%	56.50% $\pm$ 7.16%
<b>AUC, Mean <math>\pm</math> Std.</b>	69.74% $\pm$ 5.90%	47.14% $\pm$ 8.84%	54.15% $\pm$ 9.51%
<b>F1 Score, Mean <math>\pm</math> Std.</b>	55.85% $\pm$ 8.65%	39.20% $\pm$ 13.49%	42.85% $\pm$ 17.95%

Our evaluation of the relative discriminative power of features from each of the three functional networks when fused with readily available demographic information is reported in Table 6. The SVM model trained with the DMN features performs the best with a mean AUC of 80.91% and F1 score of 73.97% (averaged over the five test folds). The SVM models trained on features from the SN and ECN achieve mean AUCs of 73.59% and 79.75%, respectively, and mean F1 scores of 65.32% and 69.93%, respectively, with similar variance.

**Table 6**  
5-Fold Cross-validation Accuracy, Area under the ROC Curve (AUC), and F1 Scores for Models Trained on DMN, SN, and ECN Features Fusing Demographic Features

<b>Metric/Network</b>	<b>DMN</b>	<b>SN</b>	<b>ECN</b>
<b>Accuracy, Mean <math>\pm</math> Std.</b>	80.17% $\pm$ 18.92%	73.67% $\pm$ 17.90%	77.67% $\pm$ 17.11%
<b>AUC, Mean <math>\pm</math> Std.</b>	80.91% $\pm$ 18.73%	73.59% $\pm$ 21.60%	79.75% $\pm$ 20.64%
<b>F1 Score, Mean <math>\pm</math> Std.</b>	73.97% $\pm$ 28.52%	65.32% $\pm$ 27.21%	69.93% $\pm$ 27.26%

### 3.3 Follow-Up Analysis on Functional Hubs within the DMN

Considering the DMN is identified as the most salient and discriminative network for OUD, we conduct follow-up analysis using the Boruta ML algorithm to study the significance of features extracted from functional hubs within the DMN. Figure 7 shows the percentages of significant features ( $p$ -value  $<$  0.05) for the mPFC, PCC, ITPJ, and rTPJ. The mPFC has the highest percentage of significant features (65%) followed by the PCC (27%), ITPJ (29%), and rTPJ (23%). Table 7 reports the mean and standard deviation of feature importance rankings for each of the functional hubs with mPFC having the best (lowest) mean importance ranking, followed by ITPJ, PCC, and rTPJ.

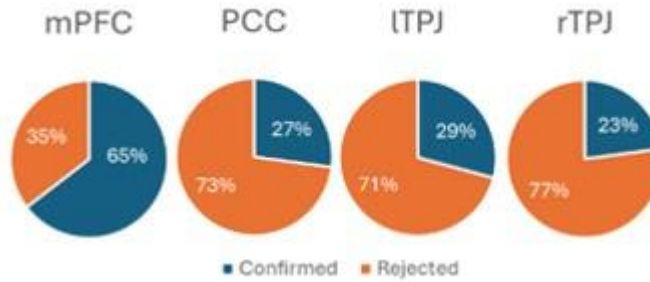


**Fig. 7.** Percentages of confirmed (significant,  $p$ -value  $< 0.05$ ) and rejected features for mPFC, PCC, ITPJ, and rTPJ functional hubs within the DMN based on our analysis using the Boruta ML algorithm.

**Table 7**

Mean and Standard Deviation of Feature Importance Rankings (Lower is Better) for mPFC, PCC, ITPJ, and rTPJ functional hubs within the DMN

DMN Functional Hub	Mean	Std.
mPFC	14.42	23.29
PCC	52.19	45.49
ITPJ	39.73	37.86
rTPJ	54.52	40.24

#### 4. Discussion

Advancing our understanding of the neurobiology underlying OUD is a crucial step towards the development of new treatment strategies to improve patient outcomes. Given its relevance across a broad range of psychopathologies, including substance use disorders, the triple network model, which includes the DMN, SN, and ECN, is a useful basis for fMRI-based study of OUD-related differences in functional brain networks. While the majority of rs-fMRI studies of OUD perform FC analyses between different areas of the brain [13-16, 18-23], our ML-based analysis instead focuses on the neural activity within each functional network as captured by the BOLD signal characteristics. Among the networks of the triple network model (DMN, SN, and ECN), our data-driven ML approach identifies the DMN as the most important functional brain network for OUD based on rs-fMRI BOLD features. This finding is supported by multiple analyses. The DMN is identified as the most significant network by the Boruta ML algorithm. Our brain activity mapping shows increased activity in the DMN for OUD. Furthermore, the DMN is the network exhibiting the greatest discriminative power in our OUD vs. HC ML classification experiments.

Our investigation of mPFC, PCC, ITPJ, and rTPJ functional hubs within the DMN suggest that all four functional hubs may be important in understanding the neurobiology of OUD. Given that mPFC is ranked the highest in feature importance (Table 7) and has the greatest percentage of significant features (Fig. 7), it may be of particular interest for future study. A prior rs-fMRI study [27] of FC also finds the PCC to be implicated in opioid abuse. Furthermore, the ITPJ and rTPJ, which have not been of particular interest for fMRI analysis, may benefit from increased attention in future research studies of OUD.

Table 8 summarizes existing works in the literature on ROI identification for OUD based on rs-fMRI. Our study's findings highlighting the DMN align with multiple previous studies that have utilized ALFF and FC to identify differences in functional networks for OUD compared to HC patients. This agreement further reinforces the role of the DMN as a critical brain network for OUD with regard to both FC and BOLD signal analysis, underscoring its potential importance in both clinical diagnosis and treatment planning. While our Boruta analysis of BOLD features finds that the ECN is not significant for distinguishing between OUD and HC, preliminary results by Woisaird et al. [21] suggest that reduced FC in the left ECN may be relevant for characterizing the neurobiology of OUD. Further studies are required to better understand the unique and complementary contributions of FC analysis and BOLD signal analysis, as well as the implications of findings for patient prognosis. Furthermore, future research is needed to investigate the extent to which the DMN, SN, and ECN and their constituent anatomical parts are implicated in OUD. Table 8 further shows that our study benefits from a greater sample size for both OUD (31) and HC (45) compared to similar prior works.

**Table 8**  
State-of-the-Art ROI Identification for OUD Based on rs-fMRI

Study	Method	#OUD	#HC	Findings
Wang et al., 2010 [13]	Seed-based FC Analysis	15 heroin-dependent individuals (HDIs)	15	The FC of the anterior cingulate cortex (ACC) of the SN is studied. HDIs show decreased connectivity of the ACC to the parahippocampal gyrus and PCC of the DMN.
Jiang et al., 2011 [24]	ALFF	24 HDIs	24	HDIs show increased ALFF in regions of the DMN and ECN, among others. HDIs show decreased ALFF in multiple regions including the bilateral dorsal anterior cingulate cortex of the SN and PCC of the DMN.
Ma et al., 2011 [18]	Independent Component Analysis	14 HDIs	13	HDIs show increased FC in the right hippocampus and decreased connectivity in right dorsal anterior cingulate cortex and left caudate in the DMN.
Liu et al., 2011 [23]	Graph Theory Analysis	16 HDIs	16	Increased FC in the medial frontal gyrus and decreased connectivity in the anterior cingulate cortex of the SN are observed for HDIs.
Li et al., 2013 [27]	Seed-based FC Analysis	14 HDIs	15	Altered connectivity in PCC-insula and PCC-striatum areas of the DMN may be regarded as biomarkers of brain damage severity in chronic heroin users.
Wang et al., 2013 [71]	ALFF	15 HDIs	15	HDIs show decreased ALFF in the right dorsal anterior cingulate cortex of the SN, as well as the right caudate and right superior medial frontal cortex. Increased ALFF is observed in bilateral cerebellum, left superior temporal gyrus and left superior occipital gyrus.
Jiang et al., 2013 [22]	Graph Theory Analysis	15 HDIs	15	For HDIs, decreased nodal centralities are observed in the ECN, including the left middle frontal gyrus and right precuneus, and increased nodal centralities are observed in the left hippocampus.
Zhang et al., 2015 [16]	Seed-based FC Analysis	21 HDIs	15	The FC of three subregions of the ACC in the SN are studied. Compared to HC, HDIs show variations in connectivity for all three subregions.
Ma et al., 2015 [15]	Seed-based FC Analysis	14 HDIs	14	Structural and FC within the DMN are disturbed in HDIs, progressing with duration of heroin use and correspond to decision making deficits.
Li et al., 2015 [19]	Independent Component Analysis	13 heroin relapsers, 13 abstainers	0	Relapsers exhibit decreased connectivity in the left inferior temporal gyrus and right superior occipital gyrus within the DMN and increased connectivity in front precuneus and right middle cingulum.
Qiu et al., 2016 [25]	ALFF	14 codeine-dependent individuals	14	Codeine-dependent individuals show decreased ALFF in multiple brain regions including the left dorsal lateral prefrontal cortex of the ECN and increased ALFF in the bilateral parahippocampal gyrus of the DMN.
Li et al., 2016 [20]	Independent Component Analysis	24 HDIs	20	Abnormal FC within the anterior subnetwork of DMN in heroin-dependent individuals is associated with basal heroin craving.
Woisard et al., 2021 [21]	Independent Component Analysis	25 OUD	25	No significant group differences are found for DMN, SN, or right ECN. Preliminary results suggest left ECN connectivity may differ between OUD and HC.
Ours	ML-based BOLD signal analysis	31 OUD	45	Multiple analyses identify the DMN as the most salient network for distinguishing between OUD and HC.

## 5. Conclusion

This study, for the first time in the literature, proposes an ML approach to identify differentiated functional brain networks for OUD using rs-fMRI BOLD signal analysis. Existing rs-fMRI studies of OUD have primarily focused on FC analyses between different areas of the brain or use average amplitude of the BOLD signal (ALFF) as a static measure of neural activity. However, emerging findings in the rs-fMRI literature suggest that BOLD signal fluctuations, e.g., BOLD signal variability, may provide insight into compensatory or suboptimal functioning of neural systems. Consequently, this study helps to understand the effect of OUD in functional brain areas using data-driven ML analysis of the BOLD signals extracted based on resting-state pseudo-events over multiple time points. Our analysis using the Boruta ML algorithm reveals that the DMN is the most salient functional network distinguishing OUD from HC with the most statistically significant rs-fMRI BOLD features. Group based analysis using brain mapping also visualizes heightened neural activity in the DMN for patients with OUD compared to HC. The results of the 5-fold ML cross-validation experiments using kernel SVM show that the DMN is the most discriminative of the three functional networks (DMN, SN, ECN), achieving a mean AUC of 80.91% and mean F1 score of 73.97% when we fuse the DMN BOLD features with demographic features. The systematic analysis and results in this study show the DMN as an active brain functional area relevant to OUD, largely agreeing with the ROI identification literature based on ALFF and FC analysis. This work further explores four functional hubs (mPFC, PCC, ITPJ, and rTPJ) within the DMN using the Boruta ML algorithm. Our approach identifies significant BOLD features for all four functional hubs, suggesting that all of these hubs may serve as targets for future OUD studies.

Future studies may validate and use these findings to generate new hypotheses for exploring the underlying neurobiology of OUD. While ML has proven to be a useful tool for a wide variety of clinical analyses, we have not seen other studies of OUD using ML for fMRI analysis. Our proposed approach and findings demonstrate the feasibility and utility of ML modeling for rs-fMRI BOLD feature analysis in OUD, which we hope will help facilitate further data-driven research aimed at understanding OUD-related changes in the brain. Further investigation will be required to understand the unique and complementary contributions of FC and data-driven ML analysis of BOLD signals over time in the resting brain with respect to OUD. Future research can build on these findings to develop more accurate and effective diagnostic and treatment strategies for OUD and other related disease conditions.

### CRedit Authorship Contribution Statement

**Ahmed Temtam:** Data curation, Formal analysis, Investigation, Methodology, Software, Visualization, Writing – original draft, Writing – review & editing. **Megan A. Witherow:** Formal analysis, Investigation, Methodology, Software, Visualization, Writing – review & editing. **Liangsuo Ma:** Data Curation, Methodology, Validation. **M. Shibly Sadique:** Software. **F. Gerard Moeller:** Funding Acquisition, Project Administration, Resources, Supervision, Validation. **Khan M. Iftekharuddin:** Conceptualization, Funding Acquisition, Project Administration, Resources, Supervision, Writing – review & editing.



## Declaration of Competing Interest

The authors declare that they have no known competing financial interests or personal relationships that could have appeared to influence the work in this paper.

## Acknowledgements

This research is supported by National Institutes of Health (NIH) - Clinical and Translational Science Awards (CTSA) Grant No. UM1TR004360.

## References

- [1] M. R. Spencer, A. M. Miniño, and M. Warner, "Drug overdose deaths in the United States, 2001–2021," *NCHS data brief*, vol. 457, pp. 1-8, 2022.
- [2] H. Hedegaard, A. M. Miniño, M. R. Spencer, and M. Warner, "Drug overdose deaths in the United States, 1999–2020," 2021.
- [3] G. C. Wide-ranging online data for epidemiologic research (WONDER). Atlanta. National Center for Health Statistics; [Online]. Available: Available at <http://wonder.cdc.gov>
- [4] K. Herlinger and A. Lingford-Hughes, "Opioid use disorder and the brain: a clinical perspective," *Addiction*, vol. 117, no. 2, pp. 495-505, 2022.
- [5] M. T. Sutherland, M. J. McHugh, V. Pariyadath, and E. A. Stein, "Resting state functional connectivity in addiction: Lessons learned and a road ahead," *Neuroimage*, vol. 62, no. 4, pp. 2281-2295, 2012.
- [6] H. Moningga, S. Lichenstein, and S. W. Yip, "Current understanding of the neurobiology of opioid use disorder: An overview," *Current behavioral neuroscience reports*, vol. 6, pp. 1-11, 2019.
- [7] H. Moningga, S. Lichenstein, P. D. Worhunsky, E. E. DeVito, D. Scheinost, and S. W. Yip, "Can neuroimaging help combat the opioid epidemic? A systematic review of clinical and pharmacological challenge fMRI studies with recommendations for future research," *Neuropsychopharmacology*, vol. 44, no. 2, pp. 259-273, 2019/01/01 2019.
- [8] J. Kakko, H. Alho, A. Baldacchino, R. Molina, F. A. Nava, and G. Shaya, "Craving in opioid use disorder: from neurobiology to clinical practice," *Frontiers in Psychiatry*, vol. 10, p. 592, 2019.
- [9] G. F. Koob, "Neurobiology of opioid addiction: opponent process, hyperkatifeia, and negative reinforcement," *Biological psychiatry*, vol. 87, no. 1, pp. 44-53, 2020.
- [10] C. J. Evans and C. M. Cahill, "Neurobiology of opioid dependence in creating addiction vulnerability," *F1000Research*, vol. 5, 2016.
- [11] L. Jin *et al.*, "Regional cerebral metabolism alterations and functional connectivity in individuals with opioid use disorder: An integrated resting-state PET/fMRI study," *Journal of Psychiatric Research*, 2023.
- [12] J. L. Stewart, S. S. Khalsa, R. Kuplicki, M. Puhl, T. Investigators, and M. P. Paulus, "Interoceptive attention in opioid and stimulant use disorder," *Addiction Biology*, vol. 25, no. 6, p. e12831, 2020.
- [13] W. Wang *et al.*, "Changes in functional connectivity of ventral anterior cingulate cortex in heroin abusers," (in eng), *Chin Med J (Engl)*, vol. 123, no. 12, pp. 1582-8, Jun 2010.
- [14] Q. Li *et al.*, "Abnormal function of the posterior cingulate cortex in heroin addicted users during resting-state and drug-cue stimulation task," (in eng), *Chin Med J (Engl)*, vol. 126, no. 4, pp. 734-9, Feb 2013.
- [15] X. Ma *et al.*, "Aberrant default-mode functional and structural connectivity in heroin-dependent individuals," *PLoS One*, vol. 10, no. 4, p. e0120861, 2015.
- [16] Y. Zhang *et al.*, "Alterations in brain connectivity in three sub-regions of the anterior cingulate cortex in heroin-dependent individuals: Evidence from resting state fMRI," (in eng), *Neuroscience*, vol. 284, pp. 998-1010, Jan 22 2015.
- [17] T. Matsui, T. Murakami, and K. Ohki, "Neuronal Origin of the Temporal Dynamics of Spontaneous BOLD Activity Correlation," *Cerebral Cortex*, vol. 29, no. 4, pp. 1496-1508, 2018.
- [18] N. Ma *et al.*, "Abnormal brain default-mode network functional connectivity in drug addicts," *PloS one*, vol. 6, no. 1, p. e16560, 2011.
- [19] W. Li *et al.*, "Dysfunctional Default Mode Network in Methadone Treated Patients Who Have a Higher Heroin Relapse Risk," *Scientific Reports*, vol. 5, no. 1, p. 15181, 2015/10/15 2015.
- [20] Q. Li *et al.*, "Disrupted default mode network and basal craving in male heroin-dependent individuals: a resting-state fMRI study," *The Journal of clinical psychiatry*, vol. 77, no. 10, p. 4560, 2016.

- [21] K. Woisard *et al.*, "Preliminary findings of weaker executive control network resting state fMRI functional connectivity in opioid use disorder compared to healthy controls," *Journal of addiction research & therapy*, vol. 12, no. 10, 2021.
- [22] G. Jiang *et al.*, "Disrupted Topological Organization in Whole-Brain Functional Networks of Heroin-Dependent Individuals: A Resting-State fMRI Study," *PLOS ONE*, vol. 8, no. 12, p. e82715, 2013.
- [23] J. Liu *et al.*, "Interaction between dysfunctional connectivity at rest and heroin cues-induced brain responses in male abstinent heroin-dependent individuals," *PLoS one*, vol. 6, no. 10, p. e23098, 2011.
- [24] G. H. Jiang *et al.*, "Amplitude low-frequency oscillation abnormalities in the heroin users: a resting state fMRI study," (in eng), *Neuroimage*, vol. 57, no. 1, pp. 149-154, Jul 1 2011.
- [25] Y. W. Qiu *et al.*, "Short-term UROD treatment on cerebral function in codeine-containing cough syrups dependent male individuals," (in eng), *Eur Radiol*, vol. 26, no. 9, pp. 2964-73, Sep 2016.
- [26] V. Scarapicchia, H. Kwan, A. Czipfel, and J. R. Gawryluk, "Differences Between Resting-State fMRI BOLD Variability and Default Mode Network Connectivity in Healthy Older and Younger Adults," (in eng), *Brain Connect*, vol. 14, no. 7, pp. 391-398, Sep 2024.
- [27] L. Qiang *et al.*, "Abnormal function of the posterior cingulate cortex in heroin addicted users during resting-state and drug-cue stimulation task," *Chinese Medical Journal*, vol. 126, no. 4, pp. 734-739, 2013.
- [28] E. Lesage and E. A. Stein, "Networks associated with reward," in *Neuroscience in the 21st Century: From Basic to Clinical*: Springer, 2022, pp. 1991-2017.
- [29] V. Menon, "Large-scale brain networks and psychopathology: a unifying triple network model," *Trends in Cognitive Sciences*, vol. 15, no. 10, pp. 483-506, 2011/10/01/ 2011.
- [30] S. W. Yip, E. E. DeVito, H. Kober, P. D. Worhunsky, K. M. Carroll, and M. N. Potenza, "Anticipatory reward processing among cocaine-dependent individuals with and without concurrent methadone-maintenance treatment: Relationship to treatment response," (in eng), *Drug Alcohol Depend*, vol. 166, pp. 134-42, Sep 1 2016.
- [31] M. Lou, E. Wang, Y. Shen, and J. Wang, "Cue-Elicited Craving in Heroin Addicts at Different Abstinent Time: An fMRI Pilot Study," *Substance Use & Misuse*, vol. 47, no. 6, pp. 631-639, 2012/04/17 2012.
- [32] M. Petersen *et al.*, "Brain network architecture constrains age-related cortical thinning," *NeuroImage*, vol. 264, p. 119721, 2022/12/01/ 2022.
- [33] F. de la Cruz, A. Schumann, S. Suttikus, N. Helbing, R. Zopf, and K.-J. Bär, "Cortical thinning and associated connectivity changes in patients with anorexia nervosa," *Translational Psychiatry*, vol. 11, no. 1, p. 95, 2021/02/04 2021.
- [34] A. M. Muller, D. L. Pennington, and D. J. Meyerhoff, "Substance-Specific and Shared Gray Matter Signatures in Alcohol, Opioid, and Polysubstance Use Disorder," (in English), *Frontiers in Psychiatry*, Original Research vol. 12, 2022-January-18 2022.
- [35] R. J. Ellis, Z. Wang, N. Genes, and A. Ma'ayan, "Predicting opioid dependence from electronic health records with machine learning," *BioData mining*, vol. 12, no. 1, pp. 1-19, 2019.
- [36] W. Farzana, Z. Shboul, A. Temtam, and K. Iftekharuddin, "Uncertainty estimation in classification of MGMT using radiogenomics for glioblastoma patients," in *Medical Imaging 2022: Computer-Aided Diagnosis*, 2022, vol. 12033, pp. 365-371: SPIE.
- [37] M. Sadique, A. Temtam, E. Lappinen, and K. Iftekharuddin, "Radiomic texture feature descriptor to distinguish recurrent brain tumor from radiation necrosis using multimodal MRI," in *Medical Imaging 2022: Computer-Aided Diagnosis*, 2022, vol. 12033, pp. 654-660: SPIE.
- [38] Z. Segal *et al.*, "Development of a machine learning algorithm for early detection of opioid use disorder," *Pharmacology Research & Perspectives*, vol. 8, no. 6, p. e00669, 2020.
- [39] A. Temtam, E. J. Cruz, H. Okhravi, D. Strock, M. Sternick, and K. M. Iftekharuddin, "Advanced machine learning approach to increase diagnostic accuracy in atypical Alzheimer's disease cases," *Alzheimer's & Dementia*, vol. 19, p. e065269, 2023.
- [40] A. Kalantari, A. Kamsin, S. Shamshirband, A. Gani, H. Alinejad-Rokny, and A. T. Chronopoulos, "Computational intelligence approaches for classification of medical data: State-of-the-art, future challenges and research directions," *Neurocomputing*, vol. 276, pp. 2-22, 2018.
- [41] F. Hamidi *et al.*, "Identifying potential circulating miRNA biomarkers for the diagnosis and prediction of ovarian cancer using machine-learning approach: application of Boruta," *Frontiers in Digital Health*, vol. 5, p. 1187578, 2023.
- [42] M. A. Witherow, N. Diawara, J. Keener, J. W. Harrington, and K. M. Iftekharuddin, "Pilot Study to Discover Candidate Biomarkers for Autism based on Perception and Production of Facial Expressions," *arXiv preprint arXiv:2404.16040*, 2024.

- [43] A. Temtam, L. Ma, F. G. Moeller, M. Sadique, and K. Iftexharuddin, "Opioid use disorder prediction using machine learning of fMRI data," in *Medical Imaging 2023: Computer-Aided Diagnosis*, 2023, vol. 12465, pp. 142-146: SPIE.
- [44] H. Feng, R. Elladki, J. Jiang, and G.-W. Wei, "Machine-learning analysis of opioid use disorder informed by MOR, DOR, KOR, NOR and ZOR-based interactome networks," *Computers in Biology and Medicine*, vol. 157, p. 106745, 2023/05/01/ 2023.
- [45] H. Feng, J. Jiang, and G.-W. Wei, "Machine-learning repurposing of DrugBank compounds for opioid use disorder," *Computers in Biology and Medicine*, vol. 160, p. 106921, 2023/06/01/ 2023.
- [46] A. Wadekar, "Predicting opioid use disorder (OUD) using a random forest," in *2019 IEEE 43rd Annual Computer Software and Applications Conference (COMPSAC)*, 2019, vol. 1, pp. 960-961: IEEE.
- [47] J. Al Faysal *et al.*, "An explainable machine learning framework for predicting the risk of buprenorphine treatment discontinuation for opioid use disorder among commercially insured individuals," *Computers in Biology and Medicine*, vol. 177, p. 108493, 2024/07/01/ 2024.
- [48] A. Acharjee, J. Larkman, Y. Xu, V. R. Cardoso, and G. V. Gkoutos, "A random forest based biomarker discovery and power analysis framework for diagnostics research," *BMC Medical Genomics*, vol. 13, no. 1, p. 178, 2020/11/23 2020.
- [49] M. B. Kursa, A. Jankowski, and W. R. Rudnicki, "Boruta – A System for Feature Selection," *Fundamenta Informaticae*, vol. 101, pp. 271-285, 2010.
- [50] J. Serrano-López *et al.*, "Machine learning applied to gene expression analysis of T-lymphocytes in patients with cGVHD," *Bone Marrow Transplantation*, vol. 55, no. 8, pp. 1668-1670, 2020/08/01 2020.
- [51] A. Chateigner *et al.*, "Gene expression predictions and networks in natural populations supports the omnigenic theory," *BMC genomics*, vol. 21, pp. 1-16, 2020.
- [52] L. Zhao, Y.-K. Sun, S.-W. Xue, H. Luo, X.-D. Lu, and L.-H. Zhang, "Identifying Boys With Autism Spectrum Disorder Based on Whole-Brain Resting-State Interregional Functional Connections Using a Boruta-Based Support Vector Machine Approach," (in English), *Frontiers in Neuroinformatics*, Original Research vol. 16, 2022-February-22 2022.
- [53] Z. Wang, X. Zhou, Y. Gui, M. Liu, and H. Lu, "Multiple measurement analysis of resting-state fMRI for ADHD classification in adolescent brain from the ABCD study," *Translational Psychiatry*, vol. 13, no. 1, p. 45, 2023/02/06 2023.
- [54] X. Zhou, Q. Lin, Y. Gui, Z. Wang, M. Liu, and H. Lu, "Multimodal MR Images-Based Diagnosis of Early Adolescent Attention-Deficit/Hyperactivity Disorder Using Multiple Kernel Learning," (in English), *Frontiers in Neuroscience*, Original Research vol. 15, 2021-September-14 2021.
- [55] G. Sansone *et al.*, "Patterns of gray and white matter functional networks involvement in glioblastoma patients: indirect mapping from clinical MRI scans," (in English), *Frontiers in Neurology*, Original Research vol. 14, 2023-June-20 2023.
- [56] J. Li, Y. Sun, Y. Huang, A. Bezerianos, and R. Yu, "Machine learning technique reveals intrinsic characteristics of schizophrenia: an alternative method," (in eng), *Brain Imaging Behav*, vol. 13, no. 5, pp. 1386-1396, Oct 2019.
- [57] R. PP, "Human experimentation. Code of ethics of the world medical association. Declaration of Helsinki," *British medical journal*, vol. 2, no. 5402, pp. 177-177, 1964.
- [58] L. Ma *et al.*, "Resting-state directional connectivity and anxiety and depression symptoms in adult cannabis users," *Biological psychiatry: cognitive neuroscience and neuroimaging*, vol. 6, no. 5, pp. 545-555, 2021.
- [59] Y. Hirano, B. Stefanovic, and A. C. Silva, "Spatiotemporal evolution of the functional magnetic resonance imaging response to ultrashort stimuli," *Journal of Neuroscience*, vol. 31, no. 4, pp. 1440-1447, 2011.
- [60] J. Martindale *et al.*, "The hemodynamic impulse response to a single neural event," *Journal of Cerebral Blood Flow & Metabolism*, vol. 23, no. 5, pp. 546-555, 2003.
- [61] T. L. Davis, K. K. Kwong, R. M. Weisskoff, and B. R. Rosen, "Calibrated functional MRI: mapping the dynamics of oxidative metabolism," *Proceedings of the National Academy of Sciences*, vol. 95, no. 4, pp. 1834-1839, 1998.
- [62] R. D. Hoge, J. Atkinson, B. Gill, G. R. Crelier, S. Marrett, and G. B. Pike, "Investigation of BOLD signal dependence on cerebral blood flow and oxygen consumption: the deoxyhemoglobin dilution model," *Magnetic Resonance in Medicine: An Official Journal of the International Society for Magnetic Resonance in Medicine*, vol. 42, no. 5, pp. 849-863, 1999.
- [63] M. E. Raichle, "Behind the scenes of functional brain imaging: a historical and physiological perspective," *Proceedings of the National Academy of Sciences*, vol. 95, no. 3, pp. 765-772, 1998.

- [64] S. Ogawa, T.-M. Lee, A. R. Kay, and D. W. Tank, "Brain magnetic resonance imaging with contrast dependent on blood oxygenation," *proceedings of the National Academy of Sciences*, vol. 87, no. 24, pp. 9868-9872, 1990.
- [65] W. D. Penny, K. J. Friston, J. T. Ashburner, S. J. Kiebel, and T. E. Nichols, *Statistical parametric mapping: the analysis of functional brain images*. Elsevier, 2011.
- [66] G.-R. Wu *et al.*, "rsHRF: A toolbox for resting-state HRF estimation and deconvolution," *NeuroImage*, vol. 244, p. 118591, 2021.
- [67] M. A. Lindquist, J. M. Loh, L. Y. Atlas, and T. D. Wager, "Modeling the hemodynamic response function in fMRI: efficiency, bias and mis-modeling," *Neuroimage*, vol. 45, no. 1, pp. S187-S198, 2009.
- [68] C. J. Keller *et al.*, "Neurophysiological Investigation of Spontaneous Correlated and Anticorrelated Fluctuations of the BOLD Signal," *The Journal of Neuroscience*, vol. 33, no. 15, pp. 6333-6342, 2013.
- [69] H. Kaneko, "Examining variable selection methods for the predictive performance of regression models and the proportion of selected variables and selected random variables," *Heliyon*, vol. 7, no. 6, p. e07356, 2021/06/01/ 2021.
- [70] E. T. Rolls, C. C. Huang, C. P. Lin, J. Feng, and M. Joliot, "Automated anatomical labelling atlas 3," (in eng), *Neuroimage*, vol. 206, p. 116189, Feb 1 2020.
- [71] Y. Wang *et al.*, "Altered fronto-striatal and fronto-cerebellar circuits in heroin-dependent individuals: a resting-state FMRI study," (in eng), *PLoS One*, vol. 8, no. 3, p. e58098, 2013.